The ozone-activated peroxymonosulfate process for the removal of a mixture of TrOCs with different ozone reactivity at environmentally relevant conditions: technical performance, radical exposure and online monitoring by spectral surrogate parameters

Emma Deniere[1]*, Herman Van Langenhove*[1]*, Stijn Van Hulle*[2]*, Kristof Demeestere*[1]

[1] Research group EnVOC, Department of Green Chemistry and Technology, Ghent University, Coupure Links 653, B-9000 Ghent, Belgium

[2] Research group LIWET, Department of Green Chemistry and Technology, Ghent University Campus Kortrijk, Sint-Martens Latemlaan 2B, B-8500 Kortrijk, Belgium

AUTHOR INFORMATION

Corresponding Author

Kristof Demeestere

E Kristof.Demeestere@UGent.be

T +32 9 264 59 65

ABSTRACT

Secondary effluent from wastewater treatment plants contains trace organic contaminants (TrOCs) that are subsequently discharged into the environment. Ozonation can offer a solution for TrOCs removal from effluent and has been extensively investigated with respect to reaction mechanisms, performance and control strategies in view of full-scale application. The ozone-activated peroxymonosulfate process (O_3/PMS) is a relatively new and promising upgrade of ozonation for which research under real conditions is, however, still lacking. Therefore, this work focuses on the removal of 11 TrOCs with different ozone reactivity at relevant environmental concentrations in effluent by using O_3/PMS. At short reaction times, the hydroxyl radical exposure is approximately 2 times higher in O_3/PMS than during ozonation at O_3 concentrations exceeding the instantaneous ozone demand (IOD). The radical production during O_3/PMS is even noticeable at ozone concentrations lower than the IOD, which indicates that radical reaction pathways are more important during the IOD phase in O_3/PMS than during ozonation. At longer reaction times, also direct PMS oxidation enhanced the removal of some TrOCs at low ozone concentrations (< IOD). However, the extra TrOCs removal during O_3/PMS is overall minimal compared to ozonation, i.e. up to 24% extra removal at the highest ozone concentrations (12.3 mg/L). In a second part of this research, spectral surrogate models based on UV absorbance at 254 nm (UVA_{254}) and fluorescence were developed for the prediction of TrOCs removal. The intensity of both surrogates decreased in a similar way as a function of the applied ozone concentration. However, the regression parameters of the surrogate models and particularly the location of the inflection point showed differences between O_3 and O_3/PMS.

Keywords: ozone, peroxymonosulfate, surrogates, UVA_{254}, fluorescence, wastewater

1. INTRODUCTION

Trace organic contaminants (TrOCs) such as pharmaceuticals, personal care products, pesticides and endocrine disrupting chemicals are found in the aquatic environment at low concentrations, i.e. ranging from ng/L to µg/L [1–3]. Wastewater treatment plants (WWTPs) have been identified as a major pathway through the discharge of secondary effluent in the environment [1]. To remove these TrOCs from the secondary effluent, a change in the design and operation of WWTPs is needed [4]. More specifically, an extra polishing step should be introduced that focuses on the removal of biorecalcitrant TrOCs. Advanced oxidation processes (AOPs) are extensively investigated [2] and ozonation (O_3) has recently been implemented in WWTPs in Switzerland and other countries for this purpose [5,6].

The mechanisms of the ozonation process are well-known, and control strategies for optimal ozone dosage have been investigated in recent years [5,7–10]. Ozonation depends on both direct ozone and indirect hydroxyl radical ($^{\bullet}$OH) reactions for the removal of TrOCs [11]. In a first phase, ozone quickly reacts with the effluent organic matter (EfOM), which initiates the production of $^{\bullet}$OH. Some TrOCs are also ozone-reactive, but their impact on the radical production is minimal in comparison to that of EfOM, given the lower concentrations at which TrOCs are present in the effluent (µg/L vs mg/L). This phase is characterized by the instantaneous ozone demand (IOD), which represents the ozone that is consumed by the highly ozone-reactive EfOM components and inorganic ozone scavengers such as nitrite [12]. Although the radicals produced during this phase can contribute to the degradation of ozone-recalcitrant TrOCs [13], this is reduced at high IOD values because of lower or delayed ●OH exposures [14,15]. Therefore, in these effluents, it is crucial that higher ozone concentrations are added to exceed the IOD value and to achieve higher TrOCs removal [5]. It is critical that the TrOC concentration or their removal can be monitored during ozone applications. However, TrOC analyses are cost- and time consuming, and cannot be used as a real-time measurement in order to make changes in ozone dosage. Therefore, the use of surrogate measurements is suggested within a monitoring strategy to observe TrOCs removal. Spectral parameters such as UV absorbance at 254 nm (UVA_{254}) and fluorescence are often investigated as surrogate parameters [5,7,9]. These parameters are easily measured on-site and are related to the water quality of the effluent. Hence, a reduction in the surrogate parameter intensity is observed as EfOM is oxidized by ozone and radicals during the process. This reduction can be correlated with the TrOCs removal. Typically, a (two-stage) linear relationship exists between the reduction in the intensity of the surrogate parameter and the TrOCs removal [5,7,9]. Correlation models are used to control the TrOCs removal in full-scale ozonation plants [16–19].

As $^{\bullet}OH$ are easily scavenged by bulk organic components in the wastewater matrix, the ozonation process has proven to be less efficient for TrOCs removal in highly loaded wastewaters compared to e.g. spiked clean water which is often used as a model matrix. For example, Souza et al. [20] observed a decrease in reaction rate for atrazine (ATZ) removal by approximately a factor of 15 in secondary effluent compared to spiked clean water. Deniere et al. [21] observed a reduction in ATZ and chloramphenicol removal of respectively 60% and 40% when changing the matrix from spiked clean water to secondary effluent. Therefore, there is an increased interest in AOPs that produce sulfate radicals ($SO_4^{\bullet-}$), as these are less scavenged by organic components due to their lower reactivity. For example, the reaction rate constant between $^{\bullet}OH$ and natural organic matter (NOM) varies between $(1.4 – 4.6) \times 10^8\ M^{-1}s^{-1}$, while the reaction rate constant between $SO_4^{\bullet-}$ and NOM is $(0.46 – 8.2) \times 10^7\ M^{-1}s^{-1}$ [22–25]. The O_3 process can be upgraded to the ozone-activated peroxymonosulfate process (O_3/PMS) which simultaneously generates both $^{\bullet}OH$ and $SO_4^{\bullet-}$ from the reaction between ozone and PMS ($k = 2.12 \times 10^4\ M^{-1}s^{-1}$) [26]. The pathway of radical formation is described below (Eq. 1-8) [26]:

$$SO_5^{2-} + O_3 \rightarrow SO_8^{2-} \qquad \text{Eq. (1)}$$

$$SO_8^{2-} \rightarrow SO_5^{\bullet-} + O_3^{\bullet-} \qquad \text{Eq. (2)}$$

$$SO_8^{2-} \rightarrow SO_4^{2-} + 2O_2 \qquad \text{Eq. (3)}$$

$$SO_5^{\bullet-} + O_3 \rightarrow SO_4^{\bullet-} + 2O_2 \qquad \text{Eq. (4)}$$

$$2SO_5^{\bullet-} \rightarrow 2SO_4^{\bullet-} + O_2 \qquad \text{Eq. (5)}$$

$$2SO_5^{\bullet-} \rightarrow S_2O_8^{2-} + O_2 \qquad \text{Eq. (6)}$$

$$O_3^{\bullet-} \rightleftarrows O^{\bullet-} + O_2 \qquad \text{Eq. (7)}$$

$$O^{\bullet-} + H_2O \rightarrow {}^{\bullet}OH + OH^- \qquad \text{Eq. (8)}$$

Most O_3/PMS research has been performed on the removal of ozone-recalcitrant TrOCs in spiked clean water, while only a few studies are available about its application in real water matrices. Sbardella et al. [27] assumed that if both radicals are in solution at the same time, organic matter will react faster with ●OH than with SO4●- making the latter less scavenged and thus more available for TrOCs removal [27]. However, it has recently been observed that $^{\bullet}OH$ are the dominant species during O_3/PMS in natural waters and wastewater [21], while mainly $SO_4^{\bullet-}$ are contributing to TrOCs removal in synthetic clean water [26,28–30]. The pH of both water matrices was similar (pH = 7.5-8.2), hence, this shift in radical contribution could not be ascribed to pH changes. It was suggested that $SO_4^{\bullet-}$ are transformed into $^{\bullet}OH$ via reactions with chloride in real waters [21]. Furthermore, competition has been noticed between PMS and organic matter for the consumption of ozone which reduced the removal efficiency of TrOCs during the O_3/PMS process [21,31]. The results discussed above were obtained at high TrOCs concentrations (approximately 1 mg/L) and the studies mostly focussed on the removal of one TrOC. Hence, knowledge is missing about the performance of O_3/PMS at low TrOCs concentrations and for mixtures of TrOCs. Furthermore, the applicability of spectral surrogate parameters to monitor TrOCs removal during the O_3/PMS process has not been investigated yet. Hence, it is unknown how the existing correlation models developed for the ozonation process will change (or not) when PMS is added and if a correct ozone dosing would be possible while using these existing correlation models.

To fill these knowledge gaps about O_3/PMS, the research goal of this study is three-fold: (1) to evaluate the performance of O_3/PMS for the removal of a mixture of TrOCs at environmentally relevant concentrations in a real water matrix, (2) to investigate the intensity reduction in spectral surrogate parameters during O_3/PMS, and (3) to develop and evaluate the applicability of surrogate models as an ozone dose control tool in O_3/PMS applications. This work is the first to investigate these research topics, in view of the practical application of the O_3/PMS process for TrOCs removal from secondary effluent. To address the research objectives, the removal efficiency of 11 TrOCs with a broad range in ozone reactivity ($0,1 \leq k_{O3}$ ($M^{-1}s^{-1}$) $\leq 10^6$, see Table S1) was investigated with both O_3/PMS and the conventional ozonation process (further denoted as O_3 and considered as a benchmark). The experiments were performed in secondary effluent spiked at realistic low µg/L levels, and a range of ozone concentrations (0.8-12.3 mg O_3/L) was added. At the same conditions, radical exposure experiments were performed to get a more in-depth view of the mechanisms of the O_3/PMS process.

2. MATERIALS AND METHODS

2.1 Chemicals

Flumequine (FLU) and ciprofloxacin (CIP) were provided by MpBio (Belgium), while metronidazole (METR), levofloxacin (LEVO) and trimethoprim (TRIM) were obtained from Fluka (Belgium). Atrazine (ATZ), chloramphenicol (CHLOR), amantadine (AMA), amitriptyline (AMI), venlafaxine (VEN), diclofenac (DFC) and p-nitrobenzoic acid (pNBA) were provided by Sigma Aldrich (Belgium), as well as ascorbic acid (AA), oxone (known as peroxymonosulfate or PMS), EDTA disodium salt ($Na_2EDTA.2H_2O$) and indigo trisulfonate (≥ 60%). Sodium bisulfite ($NaHSO_3$) and formic acid (LC-MS grade, 99%) were purchased at Fischer Scientific. HPLC grade water, methanol (MeOH) and acetonitrile were obtained from VWR (Belgium). All solutions were made in deionized water.

2.2 Experimental setup & design

Ozone was produced from oxygen by an ozone generator (up to 8 g O_3 h^{-1}, COM-AD-O2, Anseros GmbH, Germany). Ozone stock solutions (80-100 mg/L) were prepared by bubbling ozone gas (150 mL/min) through a sintered glass filter in ice-cooled deionized water [17,21,32]. A PMS stock solution was made by dissolving oxone in deionized water (20 g/L). Individual stock solutions of the 11 TrOCs were prepared at a concentration of 20 mg/L (ATZ), 500 mg/L (FLU, AMI and CHLOR) or 1 g/L (AMA, METR, VEN, CIP, LEVO, TRIM, DFC) in water. Next, a mixture of the TrOCs was prepared at a concentration of 2 mg/L in water and further used in the experiments.

The experiments were performed in secondary effluent, which was filtered – before spiking – by a 0.45 µm Whatman nylon membrane. The secondary effluent was collected from a conventional activated sludge process at the WWTP Harelbeke, Belgium (operated by Aquafin NV, Belgium) [21,33]. The characteristics of the effluent can be found in Table 1.

The experiments were performed in glass beakers, with a total working volume of 100 mL and 300 mL for respectively the radical exposure experiments and the TrOCs degradation experiments. The difference in total working volume between the two experiments is because of the higher sample volume needed for TrOCs analysis. The effluent was diluted in all experiments, i.e. 100 mL of reaction solution consists of 80 mL secondary effluent and 20 mL ozone stock solution. During the degradation experiments, 11 TrOCs were added to the matrix at a concentration of 1 µg/L. The reaction was started by the addition of ozone (O_3 process) or ozone and PMS (O_3/PMS process) to the spiked effluent. Ozone concentrations were varied between 0.8 and 12.3 mg/L, while PMS was each time added at a concentration of 64 mg/L. The PMS concentration was identical as in previous research [21,28]. Preliminary experiments with the probe compounds showed that 0.5 min and 30 min are appropriate sampling times. At 0.5 min, the comparison between ozonation and O3/PMS can be made, as O3/PMS has a faster radical production [21,28]. The sampling time of 30 min was chosen because all reactions during ozonation were finished as no further degradation of the TrOCs was noticed (results not shown). Hence, samples were taken for TrOCs, PMS and surrogate analysis at 0.5 min and 30 min. First, 5 mL of sample was quenched with MeOH and bubbled through with N_2 to remove respectively radicals and residual ozone. This sample was further used to determine the PMS concentration. Next, 30 mL of sample was taken for surrogate analysis and quenched with $NaHSO_3$ (50 mg/L). These samples were stored in the fridge (7°C) and analysed within 1 week analysis to avoid high variations in the organic matrix during storage [34]. The samples cannot be stored in the freezer (-21°C) due to the influence of freeze/thaw effects on the fluorescence intensity [34]. At last, the remaining volume in the beaker was quenched with AA and MeOH and was transferred into flasks to which $Na_2EDTA.2H_2O$

was added until 1 g/L in final solution was present. The pH was lowered to 3 by the addition of formic acid, prior to sample storage in the freezer (-18°C). In the Supplementary Information (SI-Text 1), additional information is given about the performance of different types of quenchers investigated for sampling in view of TrOCs analysis.

The radical exposure experiments were performed in a similar manner. Two radical probes, i.e. ATZ and pNBA, were added to the matrix to reach a final concentration of 100 µg/L each and were degraded via the O_3 and O_3/PMS process. Identical ozone and PMS concentrations were used as in the degradation experiments. The samples for PMS and surrogate analysis were taken as described above at 0.5 min and 30 min and stored in the fridge (7°C). Next to that, a sample was taken at 0.5 and 30 min and quenched with AA and MeOH to determine the residual radical probe concentration. These samples were stored in the freezer (-18°C) upon further analysis.

2.3 Analytical methods

2.3.1 General

The ozone concentration in the stock solutions was measured by the indigo method [35]. PMS concentrations were measured by a spectrophotometric method using potassium iodide [36].

COD and nitrite concentrations were determined spectrophotometrically using Hach cuvettes (Hach LCK 1414 and LCK 341) and a DR6000 spectrophotometer (Hach, Belgium). The alkalinity was determined according to standard methods, i.e. by titration using a pH meter (HQ40d multimeter) [37]. Chloride and sulfate concentrations were also determined according to standard methods by using a Dionex ion chromatograph, equipped with an AS14A column (150 x 3.0 mm, 5 µm) [37]. The composition of the mobile phase and regenerant is specified in Deniere et al. [21]. Turbidity was measured with a portable Hi 98703 (Hanna Instruments).

The instantaneous ozone demand (IOD) represents the rapid ozone consumption by highly ozone-reactive compounds in the matrix. IOD_{PMS} also includes the additional ozone consumption when PMS is added to the matrix. IOD and IOD_{PMS} were determined according to the method of Bader and Hoigné (1981), which involves the quenching of the reaction after 5 s by adding an indigo solution [21].

2.3.2 SPE-LC-HRMS for TrOCs analysis

The samples of the degradation experiments are brought back to room temperature before further handling. Next, the pH was adjusted to 7.0 ± 0.1 by the addition of (diluted) NaOH and formic acid solutions, and solid phase extraction (SPE) was performed on an automated GX-271 ASPEC^{TM} instrument (Gilson). Therefore, Oasis HLB cartridges (6 mL, 200 mg sorbent, Waters, Belgium) were first conditioned with MeOH (6 mL) and water (6 mL). Next, 200 mL sample was loaded on the HLB cartridge. After washing with water (18 mL) and drying with N_2, the analytes were eluted with a mixture of MeOH and acetone (50/50 (v/v)). The extract was dried under a N_2 stream before reconstitution in 1 mL 10:90 (v/v) MeOH/water with 0.1% FA and 0.01% $Na_2EDTA.2H_2O$.

The reconstituted extract was subsequently injected (10 µL) on a UHPLC reversed phase Hypersil Gold column (2.1 x 50 mm, 1.9 µm, Thermo Scientific). The mobile phase consisted of water and MeOH, both acidified with 0.1% FA, and was pumped at a flow rate of 350 µL/min (Accela 1250 pump, Thermo Scientific) through the column. The applied gradient is specified in Vergeynst et al. [3] and took 26 min. Mass spectrometric detection was performed on a hybrid quadrupole-Orbitrap HRMS (Q-

Exactive^{TM}, Thermo Scientific) equipped with a heated electrospray ionization (HESI-II) source and operating in full scan mode (120-760 m/z) at a resolving power of 70,000 at full width at half maximum at 200 m/z. The optimal HESI-II parameters are specified in Vergeynst et al. [3]. All TrOCs except CHLOR are measured in the positive ionization mode. To measure CHLOR, a switch to the negative ionization mode was made within the retention time interval 5.7 – 7.0 min.

2.3.3 HPLC-PDA analysis for ATZ and pNBA measurements

ATZ and pNBA were measured in the samples of the radical exposure experiments by use of a Surveyor HPLC system (Thermo Finnigan, Germany) coupled to a photodiode array detector (Thermo Finnigan, Germany). A Gemini C18 column (150 x 3.0 mm, 5 µm, Phenomenex) was kept at 35°C during the analysis. The mobile phase consisted of water (acidified to pH 2 by H_3PO_4) and acetonitrile, applying the gradient as detailed in Deniere et al. [21]. ATZ and pNBA were detected at a wavelength of 221 nm and 260 nm, respectively.

2.3.4 Surrogate analysis

UV-visible (UV-VIS) absorption spectra between 200 and 800 nm were obtained by using a Shimadzu UV-1601 spectrophotometer with a 1 cm quartz cuvette.

Fluorescence excitation and emission matrices (EEM) spectra were measured using a RF-5301 Shimadzu spectrofluorometer. Fluorescence intensities were measured at excitation wavelengths of 220 – 450 nm in 5 nm increments and emission wavelengths of 280 – 600 nm in 1 nm increments [17]. Raman scans of deionized water were measured at an excitation wavelength of 350 nm and emission wavelengths of 365 – 450 nm were recorded in 0.2 nm increments. These Raman measurements were used to normalize the fluorescence intensity of all spectra and to report the intensity in Raman units (R.U.). Parallel factor analysis (PARAFAC) was performed via MATLAB 9.11 using the drEEM toolbox [38]. A four-component model was validated before further use [17,39].

2.4 Calculations

2.4.1 Removal efficiencies

The removal efficiency of TrOCs (ΔTrOC) was calculated according to Equation 1.

$$\Delta\mathrm{TrOC} = 1 - \frac{[\mathrm{TrOC}]_t}{[\mathrm{TrOC}]_0} \qquad \text{(Eq. 1)}$$

For which $[\mathrm{TrOC}]_t$ is the TrOC concentration at 0.5 or 30 min and $[\mathrm{TrOC}]_0$ is the initial TrOC concentration. Similar calculations (Equation 2 and 3) were performed to determine the intensity reduction of the surrogate parameters ($\Delta\mathrm{UVA}_{254}$ and $\Delta\mathrm{Fmax}_{1\text{-}4}$). Fmax values were obtained from the PARAFAC analysis in MATLAB and represent the intensity values at peak wavelengths of the defined PARAFAC components (C1-C4).

$$\Delta\mathrm{UVA}_{254} = 1 - \frac{\mathrm{UVA}_{254;t}}{\mathrm{UVA}_{254;0}} \qquad \text{(Eq. 2)}$$

$$\Delta\mathrm{Fmax}_{1-4} = 1 - \frac{\mathrm{Fmax}_{1-4;t}}{\mathrm{Fmax}_{1-4;0}} \qquad \text{(Eq. 3)}$$

In which $\mathrm{UVA}_{254;t}$ or $\mathrm{Fmax}_{1\text{-}4;t}$ is the surrogate intensity after 0.5 or 30 min reaction time and $\mathrm{UVA}_{254;0}$ or $\mathrm{Fmax}_{1\text{-}4;0}$ is the initial surrogate intensity of the matrix.

2.4.2 Radical exposure and contribution

Radical probes were used to determine the radical exposure and contribution to TrOCs removal during the O_3/PMS process. pNBA was used as an $^{\bullet}$OH probe, as the reaction rate constants express a high reactivity with $^{\bullet}$OH (k_{OH} = 2.6 x 10^9 $M^{-1}s^{-1}$) and a low reactivity with ozone and $SO_4^{\bullet-}$ ($k_{O3} < 0.15\ M^{-1}s^{-1}$, $k_{SO4} < 10^6\ M^{-1}s^{-1}$) [40]. ATZ was used as the $SO_4^{\bullet-}$ probe, as it is reactive with both $^{\bullet}OH$ and $SO_4^{\bullet-}$ ($k_{OH} = k_{SO4} = 2.6 \times 10^9\ M^{-1}s^{-1}$). Both probes are also not reactive with PMS: (1) pNBA is unlikely to react with PMS as electron withdrawn groups ($-NO_2$) are not favourable for a non-radical reaction [41,42], and (2) ATZ reacts slowly with PMS ($k = 0.04\ M^{-1}s^{-1}$) [43]. This has also been confirmed in additional experiments discussed in SI-Text 1. The kinetic equations that describe the degradation of ATZ and pNBA can be found in SI-Text 2. The reactions with ozone (pNBA, ATZ) and $SO_4^{\bullet-}$ (pNBA) can be neglected, hence the equations can be simplified to:

$$\ln\left(\frac{[\mathrm{pNBA}]}{[\mathrm{pNBA}]_0}\right) = -\mathrm{k}_{\mathrm{OH,pNBA}} \times \int[\mathrm{OH}]\mathrm{dt} \qquad \text{(Eq. 4)}$$

$$\ln\left(\frac{[\mathrm{ATZ}]}{[\mathrm{ATZ}]_0}\right) = -\,\mathrm{k}_{\mathrm{OH,ATZ}} \times \int[\mathrm{OH}]\mathrm{dt} - \mathrm{k}_{\mathrm{SO_4,ATZ}} \times \int[\mathrm{SO_4}]\mathrm{dt} \qquad \text{(Eq. 5)}$$

As pNBA and ATZ are present as a mixture, the $^{\bullet}OH$ exposure is assumed equal for both probes. The pNBA removal is thus used to calculate the $^{\bullet}OH$ exposure ($\int[\mathrm{OH}]\mathrm{dt}$) in the matrix, while the removal of ATZ provides information about the $SO_4^{\bullet-}$ exposure ($\int[\mathrm{SO_4}]\mathrm{dt}$).

The concentration of ATZ and pNBA was 100 µg/L instead of 1 µg/L (which was used in the TrOCs degradation experiments) to increase the $^{\bullet}OH$ and $SO_4^{\bullet-}$ scavenging capacity by at least one order of magnitude without affecting the oxidation processes with the bulk components.

2.4.3 Statistical analysis

The regression analysis during analytical calibration (n = 11) was done by using the software RStudio. Statistical tests were performed by using SPSS at a 5% level of significance [44].

3. RESULTS AND DISCUSSION

3.1 Water quality parameters of the collected effluent

The characteristics of the collected effluent are shown in Table 1. These values are similar to those of previous sampled batches from the same WWTP [21], although the chloride and sulfate content are considerably higher (up to 2 times difference) this time. Chloride is one of the scavengers of $SO_4^{\bullet-}$ (k_{SO4} = 3 x 10^8 $M^{-1}s^{-1}$) in the O_3/PMS process, as well as organic matter (k_{SO4} = (0.46-8.2) x 10^7 $M^{-1}s^{-1}$) [22,25,45] of which the amount can be estimated based on the COD value. Most important ●OH scavengers are organic matter (k_{OH} = (1.4-4.6) x 10^8 $M^{-1}s^{-1}$) and alkalinity (k_{OH} = 8.5 x 10^6 $M^{-1}s^{-1}$) [10,25,45]. The concentration of metal ions (e.g. $Fe^{2+}$and Cu^{2+}) is not measured during the characterisation. It is supposed that the catalytic effect of metals on the ozonation process is negligible as low concentrations are expected [46–50].

3.2 Performance of O_3/PMS at environmentally relevant conditions

This section is focussed on (1) the radical production during both ozone-based oxidation processes (ozonation and O_3/PMS), and (2) the removal of a mixture of 11 TrOCs at low concentrations in secondary effluent. The results of the radical exposure (M.s) experiments are shown in Figure 1 (Section 3.1.1). Figures 2 (and S4) and 3 (and S5) show the removal (1-C/C_0, %) of the 11 selected TrOCs after the addition of various ozone concentrations (0.8-12.3 mg O_3/L) during ozonation and O_3/PMS at respectively 0.5 min and 30 min of reaction time. The results are discussed (Sections 3.1.2 and 3.2.2) based on the range of the applied ozone concentration in comparison with the IOD_{PMS} (5.2 mg O_3/L).

3.2.1 Radical exposure

Figure 1 shows that the total radical exposure in both processes increases at higher dosed ozone concentrations. At 0.5 min, the $^{\bullet}OH$ exposure is at average 2 times higher during O_3/PMS than during ozonation at ozone concentrations exceeding the IOD. Similar results are reported by Wert et al. [51] for the peroxone process (mass ratio O_3:H_2O_2 = 2). They found that, at ozone concentrations exceeding the IOD, the O_3/H_2O_2 process produces more $^{\bullet}OH$ than ozonation at 0.5 min as the pCBA removal was up to 5 times higher [51]. The ozonation process is thus slower in radical production in comparison to synergistic ozonation (O_3/H_2O_2 and O_3/PMS). This is also reflected in the fact that the $^{\bullet}OH$ exposure was similar (≤ 20% deviation) in O_3/PMS at 0.5 min as in ozonation at 30 min. For practical applications, O_3/PMS provides the clear advantage that wastewater can be treated at shorter contact times and hence in smaller reactors. The contribution of $SO_4^{\bullet -}$ to the overall radical exposure in O_3/PMS is maximal 13% at 0.5 min and 23% at 30 min, at ozone concentrations above the IOD. The $SO_4^{\bullet -}$ exposure in secondary effluent is thus relatively low compared to the $^{\bullet}OH$ exposure, which confirms our recent findings [21].

At 0.8 and 1.7 mg O_3/L, the total radical exposure is low ($< 3.4 \times 10^{-11}$ M.s) in both ozonation and O_3/PMS after 0.5 min of reaction. At 2.6 mg O_3/L, the overall radical exposure drastically increases in O_3/PMS, up to a value being 4.2 times higher than in ozonation. This suggests that PMS was activated by ozone, producing extra radicals (mainly $^{\bullet}OH$), even at ozone concentrations below the IOD. However, almost no $SO_4^{\bullet -}$ contribution is noticed at 0.5 min at ozone concentrations lower than 8 mg/L. The produced $SO_4^{\bullet -}$ are most likely rapidly consumed by the organic matrix or transformed into $^{\bullet}OH$ through reaction with Cl^- (Table 1, chloride 160 mg/L) [21,27,52]. At ozone concentrations higher than 8 mg/L, more $SO_4^{\bullet -}$ are produced and available for reactions with TrOCs.

After 30 min, the total radical exposure is on average 1.9 and 1.4 times higher than at 0.5 min during ozonation and O_3/PMS, respectively. Hence, extended contact times are more a requisite for ozonation. At low ozone concentrations (< 4.3 mg/L), the total radical exposure in O_3/PMS was up to 8 times higher than the $^{\bullet}OH$ exposure during ozonation. This is remarkable as the low concentrations of ozone (< 4.3 mg/L) are quickly consumed by the matrix and PMS at 0.5 min (see Figure S4), resulting in negligible residual ozone concentrations at longer reaction times. Hence, no extra radical formation was expected at higher reaction times. A possible explanation is that a reaction between PMS and some components in the organic matter took place, resulting in the production of extra $SO_4^{\bullet-}$ which can be transformed into $^{\bullet}OH$ via reaction with Cl^- [53]. This is advantageous as residual PMS can offer some oxidation potential without being activated by ozone.

3.2.2 TrOCs removal at applied ozone concentrations below IOD_{PMS}

The ozone-reactive TrOCs (k_{O3} > 1000 $M^{-1}s^{-1}$) achieve complete removal at ozone concentrations just below the IOD and IOD_{PMS} (i.e. respectively 4.2 and 5.2 mg O_3/L), while the removal efficiency of ozone-recalcitrant TrOCs (k_{O3} < 1000 $M^{-1}s^{-1}$) was not higher than 65% during both processes and at both reaction times.

Small differences were noticed between the removal patterns of the different TrOCs in both processes, depending on their ozone reactivity. At 0.5 min (Figure 2), the removal efficiencies of CHLOR, ATZ, FLU, AMA and METR were up to 19% higher during ozonation than during O_3/PMS. Especially for ATZ and CHLOR, ozone concentrations of at least 3.8 mg/L were needed to observe any removal with O_3/PMS, whereas already higher removal was noticed during ozonation at lower ozone concentrations. However, at the same reaction time and at 0.8 mg O_3/L, O_3/PMS shows to be more efficient (up to 27% higher removal than with ozonation) for the ozone-reactive TrOCs (AMI, VEN, CIP, LEVO, TRIM and DFC). At ozone concentrations equal to IOD and IOD_{PMS}, the TrOCs removal is approximately the same (i.e. less than 8% difference) for both processes, or slightly higher with ozonation for the ozone-reactive compounds. From these observations, two important points of attention can be addressed. First, ozone-recalcitrant TrOCs depend on radical reactions for their removal. Hence, the lower removal efficiencies during O_3/PMS suggest that less radicals were available during O_3/PMS at 0.5 min, in comparison with ozonation. However, higher total radical exposures during O_3/PMS were noticed when applying ozone concentrations equal to or higher than 2.6 mg O_3/L (Figure 1a). This suggests that the main pathway of radical formation is via PMS (and not via bulk organic matter as in ozonation) which explains the higher observed total radical exposure. However, it appears that the (in)organic matrix highly scavenges these radicals, resulting in lower TrOCs removal efficiencies in comparison to ozonation. This might be caused by the fact that the (in)organic matrix encounters less direct ozone reactions during O_3/PMS than in ozonation, which results in more residual ozone-reactive organic bulk compounds. These organic compounds are also highly reactive towards $SO_4^{\bullet -}$ and $^{\bullet}OH$, which leads to a higher scavenging capacity for radicals [27]. Wert et al. [51] made a similar observation for the O_3/H_2O_2 process, i.e. ozonation showed 10-40% higher $^{\bullet}OH$ exposure than O_3/H_2O_2 in waters with high $^{\bullet}OH$ scavenging rate, leading to a reduced pCBA removal during O_3/H_2O_2 in comparison to ozonation.

Second, in O_3/PMS, the ozone exposure of TrOCs is reduced at all ozone concentrations due to the extra ozone consumption by PMS. Nonetheless, highly ozone-reactive TrOCs were more efficiently removed during O_3/PMS, compared to ozonation, at low ozone concentrations. This indicates that these compounds were also removed by radical pathways, as the reaction (0.5 min) was too short for removal through direct PMS oxidation [54]. Sbardella et al. [27] noticed that competition for $SO_4^{\bullet -}$ occurs between pharmaceuticals and the electron-rich moieties of EfOM at low oxidant doses. Produced $SO_4^{\bullet -}$ during this phase can thus be consumed by the highly ozone-reactive TrOCs and EfOM.

Similar removal patterns are observed for the low ozone-reactive TrOCs after 30 min of reaction (Figure 3), compared to 0.5 min. For some ozone-reactive TrOCs, more pronounced differences between both processes are noticed at 30 min. For example, for CIP and LEVO, O_3/PMS reached respectively 67% and 98% removal at 0.8 mg O_3/L, while this was only 25% and 36% with ozonation. As the added ozone concentration is lower than the IOD of the secondary effluent, the ozone is completely consumed by the (in)organic matrix (see Figure S4). Consequently, the absence of residual ozone and radicals is expected which makes it hard to understand the higher removal efficiencies at 30 min than at 0.5 min of reaction time during O_3/PMS. Therefore, the impact of direct PMS reactions with the 11 selected TrOCs was investigated (Figure S3). LEVO and CIP show to be the most susceptible to PMS reactions, as at least 60% removal is observed after 30 min. Recent literature confirms that fluoroquinolones, except flumequine, are susceptible for (unactivated) PMS oxidation [55,56]. Hence, their removal does not solely depend on reactions with $^{\bullet}OH$, $SO_4^{\bullet -}$ or singlet oxygen ($^1O_2$), but for example LEVO is primarily oxidized by PMS through O-addition and dealkylation pathways [56]. Direct oxidation pathways by PMS can thus play an important role during the removal of some TrOCs at low ozone concentrations (< IOD) and extended reaction times. However, at full-scale applications of O_3/PMS, higher ozone doses (> IOD) and short reaction times (0.5 min) will be most likely used which means that PMS oxidation will only be relevant for residual oxidation, for example in pipes.

3.2.3 TrOCs removal at applied ozone concentrations exceeding IOD_{PMS}

The highly ozone-reactive TrOCs were completely removed at ozone concentrations exceeding IOD_{PMS}, in both processes and at both reaction times. FLU and AMA only obtained complete removal (95%) at the highest ozone concentration (12.3 mg O_3/L), while the removal efficiency of ATZ, CHLOR and METR was up to 54%, 75% and 90% during both processes and at both reaction times.

The removal efficiency of CHLOR, ATZ, AMA and METR was higher during O_3/PMS than during ozonation at 0.5 min and at ozone concentrations exceeding IOD_{PMS}. For example, at 12.3 mg O_3/L, the difference in removal efficiency between both processes was 24 ± 4 %, 18 ± 14 %, 6 ± 1% and 10 ± 5%, respectively. Thus, at short reaction times and for ozone-recalcitrant TrOCs, the added value of PMS is noticeable at ozone concentrations higher than IOD_{PMS}, which can be explained by the clearly higher radical production (Figure 1A) resulting from the activation of PMS at increased ozone concentrations. This agrees with our previous research at higher (order of mg/L) TrOC concentrations [21]: the increase in ATZ and CHLOR removal was 9% and 12% during O_3/PMS in comparison to ozonation, at 0.5 min and high ozone dosages (≥ 10 mg/L). Furthermore, one of the conclusions of [8] is that the synergetic effect of H_2O_2 in the peroxone process (O_3/H_2O_2) only occurs when the applied ozone concentration exceeds the IOD of the matrix [8], which is similar tat o the results of this work. The added value of PMS is the most pronounced for TrOCs that are highly recalcitrant during ozonation. So the highest impact of PMS addition is seen for ATZ and CHLOR, which could be removed for respectively 54 ± 11% and 72 ± 2% during O_3/PMS, after

0.5 min at 12.3 mg O_3/L. At 30 min, the added value of O_3/PMS compared to ozonation was no longer noticeable, even for the ozone-recalcitrant ATZ and CHLOR (less than 3% difference at 12.3 mg O_3/L), despite the higher radical exposure for O_3/PMS shown in Figure 1B. The study of Wert et al. [51] found similar results at ozone concentrations exceeding the IOD, i.e. similar $^{\bullet}OH$ exposures were noticed during ozonation after 10 min as during O_3/H_2O_2 after 0.5 min. The organic matrix promotes the radical production during ozonation at higher reaction times [8], which leads to similar TrOCs removal compared to O_3/PMS. However, these similar removal efficiencies suggest that a part of the produced radicals during O_3/PMS are scavenged by the organic matter instead of being used for TrOCs removal.

3.3 Surrogate intensity decrease and its correlation to TrOCs removal

3.3.1 Surrogate intensity decrease

UVA_{254} was chosen as a surrogate representing the electron rich aromatic or conjugated double bond moieties, which are both susceptible for ozone and $SO_4^{\bullet-}$ induced reactions [27]. Zhang et al. [57] identified fast reacting chromophores within different DOM (dissolved organic matter) fractions. The reaction rate constants with $SO_4^{\bullet}$ (k_{SO4}) for these fractions are in the order of 10^8 $M^{-1}s^{-1}$, while the highest reported reaction rate constant with ozone (k_{O3}) for DOM fractions is in the order of 10^7 $M^{-1}s^{-1}$ [10]. With respect to the fluorescence data, four PARAFAC components (C1-C4) were identified. C1, C2 and C3 are linked to humic- and fulvic-like compounds, while C4 represents soluble microbial by-products (Table 2 and Figure S5).

Figure 4 shows the decrease of UVA_{254} and $Fmax_1$ (ΔUVA_{254} and $\Delta Fmax_1$) at different ozone doses during ozonation and O_3/PMS. The same type of data for $Fmax_2$, $Fmax_3$ and $Fmax_4$ is shown in Supplementary Information (Figure S6) and, as compared with

$Fmax_1$, the same conclusions can be made. The fluorescence components are more easily degraded than UVA_{254} as e.g. approximately 20% of the fluorescence components is removed at 0.8 mg O_3/L during O_3/PMS, while no reduction was noticed for UVA_{254}. The intensity of both surrogate parameters decreased to a larger extent when applying increasing ozone concentrations. However, two regions can be distinguished with a different behaviour. In a first phase, a steep increase in ΔUVA_{254} and $\Delta Fmax_{1-4}$ is noticed as a function of the applied ozone concentration, while a smaller slope was noticed in the second phase. Table S4 summarizes the slopes and intercepts of the linear relationships in the two regions. For all 4 fluorescence surrogates, the slope of the first phase was 3.6 – 6.0 times higher compared to that of the second phase. For UVA_{254}, the difference was a factor of 1.8 – 3.3 since the slope of the second phase is higher than for the fluorescence surrogates. This means that UVA_{254} is more sensitive than Fmax to the applied ozone concentrations above the inflection point .

Furthermore, the location of the inflection point is at approximately 4.2 mg O_3/L, which corresponds to the IOD of the effluent. Hence, the highly ozone-reactive DOM moieties that absorb in the fluorescence and UV region are quickly degraded at ozone concentrations lower than IOD, which caused a strong reduction in the surrogate parameter at increasing ozone concentrations. At ozone concentrations exceeding the IOD, less ozone-reactive organic moieties are still present or produced from the previous phase, which explains the slower reduction in the surrogate parameter. This confirms the important role of the IOD with respect to surrogate intensity decrease [14,19,21].

In Figure S7, the intensity changes of the surrogate parameters during O_3/PMS are plotted versus those during ozonation. Table S5 reports the linear regression parameters of these graphs. For all surrogates and at both reaction times, except for $Fmax_1$ at 30 min, the intercept is not statistically significant ($p < 0.05$). The slope varies between 0.92 and 1.03, with one outlier of 0.83 for $Fmax_1$ at 30 min. As these slopes are almost equal to 1 and the intercept is not significant, it can be concluded that the decrease in UVA_{254} and $Fmax_{1-4}$ during both processes is similar at both reaction times. As the ozone exposure towards the bulk organic matter is lower during O_3/PMS (due to the addition of PMS), it was expected to observe a difference in the ΔUVA_{254} and $\Delta Fmax_{1-4}$ results between both ozone-based processes. However, the lack of this observation suggests that the produced radicals during O_3/PMS decrease these surrogates to a similar extent as ozone does in the ozonation process.

3.3.2 Surrogate-based prediction of TrOCs removal

Figure 5-6 and Figure S9-S11 show the relationship between TrOCs removal (ΔTrOC, %) and the intensity reduction of the surrogate parameters (ΔUVA_{254} and $\Delta Fmax_{1-4}$, %) during ozonation and O_3/PMS both at 0.5 min and 30 min reaction times. A complete removal of the most ozone-reactive TrOCs (LEVO, TRIM and DFC) was reached at a ΔUVA_{254} of 21-22% (ozonation) and 0-31% (O_3/PMS) and at a $\Delta Fmax_1$ of 41-55% (ozonation) and 20-60% (O_3/PMS), considering both time points. The TrOCs with moderate ozone activity (AMI, VEN and CIP) reached complete removal at a higher surrogate intensity decrease, i.e. at a ΔUVA_{254} of 22-44% (ozonation) and 19-46% (O_3/PMS) and at a $\Delta Fmax_1$ of 55-65% (ozonation) and 48-70% (O_3/PMS). The ozone-recalcitrant TrOCs ($k_{O3} < 1000\ M^{-1}s^{-1}$) are removed up to 96% within a ΔUVA_{254} range of 65-78% (ozonation) and 78-94% (O_3/PMS) and a $\Delta Fmax_1$ range of 85-90% (ozonation) and 82-89% (O_3/PMS).

The relationship between ∆TrOC and the surrogate intensity reduction was the best described by two linear curves. For the components with a low ozone reactivity (k_{O3} < 1000 $M^{-1}s^{-1}$), this results in a moderate slope in the first phase and a steep slope in the second phase (up to 31 times higher). On the other hand, for highly and moderate ozone-reactive TrOCs (k_{O3} ≥ 1000 $M^{-1}.s^{-1}$), a steep slope in the first phase and a moderate slope in the second phase (up to 9 times smaller) was noticed. This profile has been earlier reported for ozonation [5,17] and is confirmed in this work for the O_3/PMS process. The inflection point was determined by minimizing the mean squared error between the predicted and experimental data, while also minimizing the (prediction) difference (∆y) between the two curves at the inflection point [17]. The location of the inflection point for the different surrogates is summarized in Table 3.

Two observations suggest that the first phase in the correlation model between surrogate and TrOCs removal is dominated by the fast reactions occurring within the IOD phase of ozonation and O_3/PMS. First, the TrOCs with high and moderate ozone reactivity (k_{O3} ≥ 1000 $M^{-1}.s^{-1}$) obtain a removal efficiency of at least 90% in both processes during this first phase. Second, results shown in Figure 4 reveal that up to 40% UVA_{254} and 65% $Fmax_1$ is removed during the IOD phase of the processes, which means that the inflection points observed in Figures 5 and 6 are located before the IOD is reached.

The inflection points of the UVA_{254} correlation models at both sampling times are located at a higher value in O_3/PMS than in ozonation, while the opposite is observed in the fluorescence models. According to Chys et al. [17] the region before the inflection point is a representation of the fast direct ozone reactions that takes place during the ozonation process, while the second phase is more related to $^{\bullet}OH$ reactions. As direct ozone reactions are reduced in O_3/PMS due to ozone consumption of PMS, other (radical) reaction pathways become more dominant during that first phase. At 0.5 min, more radicals were produced during the IOD phase in O_3/PMS compared to ozonation (Figure 1a). Thus, the higher inflection point in O_3/PMS indicates that the UVA_{254} surrogate intensity decreased to a larger extent by radicals than by ozone to obtain an equal removal of > 90% of the highly and moderate ozone-reactive TrOCs (k_{O3} > 1000 $M^{-1}s^{-1}$). The fluorescence surrogates have lower removal efficiencies, which suggests that the fluorophores are less susceptible for radical reactions.

At 30 min, also direct reactions with PMS might become important. However, direct PMS oxidation appeared to have more impact on the TrOCs removal (as was seen for some TrOCs like CIP and LEVO (Figure S3) than on the surrogate removal (Figure 4). If the comparison is made between the models of O_3/PMS at 0.5 min and 30 min, it is noticed that the inflection point has a lower value in the fluorescence models and a similar value in the UVA_{254} models. This means that the control range of the first phase can be reduced in the fluorescence models using PMS. As this phase takes place at ozone concentrations below the IOD, the second phase will be of higher importance due to the higher radical production at ozone concentrations exceeding the IOD. Large control ranges within the reduction of a surrogate parameter are more favourable, as it provides a higher sensitivity for the prediction of TrOCs removal.

Hence, the second phase is the most useful to predict the removal of ozone-recalcitrant TrOCs as almost complete removal was already obtained for TrOCs with a k_{O3} of at least 8 $M^{-1}s^{-1}$. At 0.5 min, the slopes of the linear relationships are more similar among the different TrOCs during O_3/PMS than during ozonation. For example, the relative standard deviation (RSD, %), calculated for the slopes in the second phase of the 5 ozone-recalcitrant TrOCs, are 46% and 48% in respectively the UVA_{254} and $Fmax_1$-based correlation model during the ozonation process, while these values were only

13% and 17% during O_3/PMS. This smaller variation is advantageous for the prediction of the TrOCs removal, as the value of the slope can be seen as a constant which simplifies the data processing. The surrogate models of the ozonation process also show this advantage, but at longer reaction times (30 min). For example, the RSD value of the slopes is 22% for both UVA_{254} and $Fmax_1$-based correlation models during ozonation at 30 min. An explanation for these differences in reaction time can be found in the radical production. As seen in Figure 1, similar radical exposures were obtained between O_3/PMS at 0.5 min and ozonation at 30 min. The ozonation process needs longer reaction times to produce radicals, while O_3/PMS has a fast radical production due to the reaction between ozone and PMS. Hence, the surrogate-based prediction models can be applied with high accuracy at short reaction times (0.5 min) during O_3/PMS, but not during ozonation.

All these observations show the need for specific surrogate-based prediction models for the O_3/PMS process. If not, using the prediction models of the ozonation process will result in under- or overpredicting the required ozone concentration. For example, if 50% ATZ and CHLOR removal is targeted by O_3/PMS, and we assume a reaction time of 0.5 min, the model of ozonation will predict 1.7 (ATZ) and 1.3 (CHLOR) times higher ΔUVA_{254} values (and thus higher ozone concentrations) than that are needed during O_3/PMS. However, if for ozonation the correlation model is used at 30 min reaction time, it will underestimate the needed ozone concentration and thus a lower TrOCs removal.

4. CONCLUSIONS

This work has investigated for the first time the performance of the O_3/PMS process for the removal of a broad range of selected TrOCs at environmentally relevant conditions. The reaction between ozone and PMS already takes place within the IOD phase, which indicates a high level of competition between PMS and bulk organic matter for the consumption of ozone. After 0.5 min of reaction and at ozone concentrations exceeding the IOD, the total radical exposure in O_3/PMS was already at the same level as after 30 min of conventional ozonation. Hence, the O_3/PMS process shows better removal efficiencies for ozone-recalcitrant TrOCs at short reaction times (0.5 min) and at ozone concentrations exceeding the IOD of the effluent. This is advantageous in terms of reactor design, as smaller reactors and contact times can be applied. The fast ozone-reactive TrOCs have a similar removal efficiency in ozonation and O_3/PMS at 0.5 min. However, the increase in removal efficiency for all TrOCs during O_3/PMS is limited (up to 24% at 12.3 mg O_3/L) in comparison to ozonation. The process should still be optimized to achieve higher TrOCs removal during O_3/PMS in comparison to ozonation, in order to increase its added value for implementation in practice. For example, previous research has shown that the TrOC removal can be enhanced by adapting the ozone dosing strategy from one-time dosing to sequential dosing [58]. Further research could focus on optimizing the dosing strategy, on the type of scavenging reactions in effluent, and on appropriate techniques to reduce scavenging (e.g. by use of pre-filtration techniques).

Next to that, this work demonstrates that – also for the O_3/PMS process – spectral surrogates, i.e. ΔUVA_{254} and ΔFmax (fluorescence), have the potential to be used in ozone dosage control strategies to maintain a certain TrOCs removal. The established correlation models are most efficiently used in differential ozone dosage control strategies, taking into account the load, scavenging capacity and reactivity of the water matrix, which can highly influence the efficiency of TrOCs removal [5]. In future research, the correlation models could even be extended to predict the radical scavenging capacity using surrogate measurements [59], and should be validated with different secondary effluents. The intensity of both surrogates decreased in a similar way in both the ozonation and O_3/PMS process, which indicates that the extra radicals that were produced in O_3/PMS do not result in additional removal of chromophores and fluorophores. However, some differences were noticed in the surrogate models developed to predict TrOCs removal, which makes the correlations not interchangeable between ozonation and O_3/PMS. TrOCs removal

Funding sources

This research received financial support from Ghent University. Also, the financial support from the Hercules Foundation (Flemish Government; AUGE/11/016) and from the Special Research Fund of Ghent University (01B07512) is acknowledged for the UHPLC-Q-Exactive^{TM} and the automated SPE equipment, respectively.

Acknowledgments

The authors would like to thank Nathan Vannevel, Tine D’hamers, Fien Van Raemdonck, Britt Van Mieghem and Charlotte Van de Voorde for their help during the experimental work. We are also grateful to Patrick De Wispelaere for his technical support during LC-HRMS analysis. The EnVOC research group is part of the Ghent University expertise centre MSsmall.

REFERENCES

[1] J. Rogowska, M. Cieszynska-Semenowicz, W. Ratajczyk, L. Wolska, Micropollutants in treated wastewater, Ambio. 49 (2020) 487–503. https://doi.org/10.1007/s13280-019-01219-5.

[2] D. Kanakaraju, B.D. Glass, M. Oelgemöller, Advanced oxidation process-mediated removal of pharmaceuticals from water: A review, J. Environ. Manage. 219 (2018) 189–207. https://doi.org/10.1016/J.JENVMAN.2018.04.103.

[3] L. Vergeynst, K. K'oreje, P. De Wispelaere, L. Harinck, H. Van Langenhove, K. Demeestere, Statistical procedures for the determination of linearity, detection limits and measurement uncertainty: A deeper look into SPE-LC-Orbitrap mass spectrometry of pharmaceuticals in wastewater, J. Hazard. Mater. 323 (2017) 2–10. https://doi.org/10.1016/J.JHAZMAT.2016.05.077.

[4] S. de Boer, J. González-Rodríguez, J.J. Conde, M.T. Moreira, Benchmarking tertiary water treatments for the removal of micropollutants and pathogens based on operational and sustainability criteria, J. Water Process Eng. 46 (2022) 102587. https://doi.org/10.1016/J.JWPE.2022.102587.

[5] E. Deniere, M. Chys, W. Audenaert, I. Nopens, H. Van Langenhove, S. Van Hulle, K. Demeestere, Status and needs for online control of tertiary ozone-based water treatment: use of surrogate correlation models for removal of trace organic contaminants, Rev. Environ. Sci. Biotechnol. 20 (2021) 297–331. https://doi.org/10.1007/s11157-021-09574-0.

[6] W. Audenaert, M. Chys, & S.V.H.-I.-P.A. conference, U. 2014, S. Van Hulle, (Future) regulation of trace organic compounds in WWTP effluents as a driver of advanced wastewater treatment, in: IOA-PAG Annu. Conf. Expo Ozone

Proven Solut. to Emerg. Challenges, International Ozone Association-Pan America Group (IOA-PAG), 2014. https://biblio.ugent.be/publication/5714376 (accessed September 25, 2019).

[7] N. Walpen, A. Joss, U. von Gunten, Application of UV absorbance and electron-donating capacity as surrogates for micropollutant abatement during full-scale ozonation of secondary-treated wastewater, Water Res. 209 (2022) 117858. https://doi.org/10.1016/J.WATRES.2021.117858.

[8] Q.Y. Wu, Z.W. Yang, Y. Du, W.Y. Ouyang, W.L. Wang, The promotions on radical formation and micropollutant degradation by the synergies between ozone and chemical reagents (synergistic ozonation): A review, J. Hazard. Mater. 418 (2021) 126327. https://doi.org/10.1016/J.JHAZMAT.2021.126327.

[9] Z.M. Song, Y.L. Xu, J.K. Liang, L. Peng, X.Y. Zhang, Y. Du, Y. Lu, X.Z. Li, Q.Y. Wu, Y.T. Guan, Surrogates for on-line monitoring of the attenuation of trace organic contaminants during advanced oxidation processes for water reuse, Water Res. 190 (2021) 116733. https://doi.org/10.1016/J.WATRES.2020.116733.

[10] C. Von Sonntag, U. von Gunten, Chemistry of Ozone in Water and Wastewater Treatment, IWA publishing, 2012.

[11] T. Nöthe, H. Fahlenkamp, C. Von Sonntag, Ozonation of wastewater: Rate of ozone consumption and hydroxyl radical yield, Environ. Sci. Technol. 43 (2009) 5990–5995. https://doi.org/10.1021/ES900825F/SUPPL_FILE/ES900825F_SI_001.PDF.

[12] H.S. Park, T.M. Hwang, J.W. Kang, H. Choi, H.J. Oh, Characterization of raw water for the ozone application measuring ozone consumption rate, Water Res. 35 (2001) 2607–2614. https://doi.org/10.1016/S0043-1354(00)00564-9.

[13] Y. Guo, H. Wang, B. Wang, S. Deng, J. Huang, G. Yu, Y. Wang, Prediction of micropollutant abatement during homogeneous catalytic ozonation by a chemical kinetic model, Water Res. 142 (2018) 383–395. https://doi.org/10.1016/J.WATRES.2018.06.019.

[14] A. Cruz-Alcalde, S. Esplugas, C. Sans, Abatement of ozone-recalcitrant micropollutants during municipal wastewater ozonation: Kinetic modelling and surrogate-based control strategies, Chem. Eng. J. 360 (2019) 1092–1100. https://doi.org/10.1016/j.cej.2018.10.206.

[15] M.G. Antoniou, G. Hey, S. Rodríguez Vega, A. Spiliotopoulou, J. Fick, M. Tysklind, J. la Cour Jansen, H.R. Andersen, Required ozone doses for removing pharmaceuticals from wastewater effluents, Sci. Total Environ. 456–457 (2013) 42–49. https://doi.org/10.1016/j.scitotenv.2013.03.072.

[16] M. Stapf, U. Miehe, M. Jekel, Application of online UV absorption measurements for ozone process control in secondary effluent with variable nitrite concentration, Water Res. 104 (2016) 111–118. https://doi.org/10.1016/j.watres.2016.08.010.

[17] M. Chys, W.T.M. Audenaert, E. Deniere, S.T.F.C. Mortier, H. Van Langenhove, I. Nopens, K. Demeestere, S.W.H. Van Hulle, Surrogate-Based Correlation Models in View of Real-Time Control of Ozonation of Secondary Treated Municipal Wastewater—Model Development and Dynamic Validation, Environ. Sci. Technol. 51 (2017) 14233–14243. https://doi.org/10.1021/acs.est.7b04905.

[18] M. Chys, W.T.M. Audenaert, J. Vangrinsven, M. Bauwens, S.T.F.C. Mortier, H. Van Langenhove, I. Nopens, K. Demeestere, S.W.H. Van Hulle, Dynamic validation of online applied and surrogate-based models for tertiary ozonation

on pilot-scale, Chemosphere. 196 (2018) 494–501. https://doi.org/10.1016/j.chemosphere.2017.12.168.

[19] K. Chon, E. Salhi, U. von Gunten, Combination of UV absorbance and electron donating capacity to assess degradation of micropollutants and formation of bromate during ozonation of wastewater effluents, Water Res. 81 (2015) 388–397. https://doi.org/10.1016/j.watres.2015.05.039.

[20] B.S. Souza, R.F. Dantas, A. Cruz, C. Sans, S. Esplugas, M. Dezotti, Photochemical oxidation of municipal secondary effluents at low H2O2 dosage: Study of hydroxyl radical scavenging and process performance, Chem. Eng. J. 237 (2014) 268–276. https://doi.org/https://doi.org/10.1016/j.cej.2013.10.025.

[21] E. Deniere, R. Prasath Alagappan, H. Van Langenhove, S. Van Hulle, K. Demeestere, The ozone-activated peroxymonosulfate process (O3/PMS) for removal of trace organic contaminants in natural and wastewater: Effect of the (in)organic matrix composition, Chem. Eng. J. 430 (2022) 133000. https://doi.org/https://doi.org/10.1016/j.cej.2021.133000.

[22] S. Giannakis, K.A. Lin, F. Ghanbari, A review of the recent advances on the treatment of industrial wastewaters by sulfate radical-based Advanced Oxidation Processes (SR- AOPs), Chem. Eng. J. In Press (2020) 127083. https://doi.org/10.1016/j.cej.2020.127083.

[23] Y. Ahn, D. Lee, M. Kwon, I. Choi, S.-N. Nam, J.-W. Kang, Characteristics and fate of natural organic matter during UV oxidation processes, Chemosphere. 184 (2017) 960–968. https://doi.org/https://doi.org/10.1016/j.chemosphere.2017.06.079.

[24] Y. Mao, H. Dong, S. Liu, L. Zhang, Z. Qiang, Accelerated oxidation of iopamidol by ozone/peroxymonosulfate (O3/PMS) process: Kinetics,

mechanism, and simultaneous reduction of iodinated disinfection by-product formation potential, Water Res. 173 (2020) 115615. https://doi.org/10.1016/j.watres.2020.115615.

[25] M.Y. Lee, W.L. Wang, Y. Du, Q.Y. Wu, N. Huang, Z. Bin Xu, H.Y. Hu, Comparison of UV/H2O2 and UV/PS processes for the treatment of reverse osmosis concentrate from municipal wastewater reclamation, Chem. Eng. J. 388 (2020) 124260. https://doi.org/10.1016/j.cej.2020.124260.

[26] Y. Yang, J. Jiang, X. Lu, J. Ma, Y. Liu, Production of Sulfate Radical and Hydroxyl Radical by Reaction of Ozone with Peroxymonosulfate: A Novel Advanced Oxidation Process, Environ. Sci. Technol. 49 (2015) 7330–7339. https://doi.org/10.1021/es506362e.

[27] L. Sbardella, I. Velo-Gala, J. Comas, I. Rodríguez-Roda Layret, A. Fenu, W. Gernjak, The impact of wastewater matrix on the degradation of pharmaceutically active compounds by oxidation processes including ultraviolet radiation and sulfate radicals, J. Hazard. Mater. 380 (2019). https://doi.org/10.1016/j.jhazmat.2019.120869.

[28] E. Deniere, S. Van Hulle, H. Van Langenhove, K. Demeestere, Advanced oxidation of pharmaceuticals by the ozone-activated peroxymonosulfate process: the role of different oxidative species, J. Hazard. Mater. 360 (2018) 204–213. https://doi.org/10.1016/j.jhazmat.2018.07.071.

[29] J. Cong, G. Wen, T. Huang, L. Deng, J. Ma, Study on enhanced ozonation degradation of para-chlorobenzoic acid by peroxymonosulfate in aqueous solution, Chem. Eng. J. 264 (2015) 399–403. https://doi.org/10.1016/j.cej.2014.11.086.

[30] Z. Yuan, M. Sui, B. Yuan, P. Li, J. Wang, J. Qin, G. Xu, Degradation of

ibuprofen using ozone combined with peroxymonosulfate, Environ. Sci. Water Res. Technol. 3 (2017) 960–969. https://doi.org/10.1039/c7ew00174f.

[31] Z.-W. Yang, W.-L. Wang, M.-Y. Lee, Q.-Y. Wu, Y.-T. Guan, Synergistic effects of ozone/peroxymonosulfate for isothiazolinone biocides degradation: Kinetics, synergistic performance and influencing factors, Environ. Pollut. 294 (2022) 118626. https://doi.org/10.1016/J.ENVPOL.2021.118626.

[32] Z. Liu, K. Demeestere, S. Van Hulle, Pretreatment of Secondary Effluents in View of Optimal Ozone-Based AOP Removal of Trace Organic Contaminants: Bench-Scale Comparison of Efficiency and Energy Consumption, Ind. Eng. Chem. Res. 59 (2020) 8112–8120. https://doi.org/10.1021/acs.iecr.0c01210.

[33] M. Chys, K. Demeestere, I. Nopens, W.T.M. Audenaert, S.W.H. Van Hulle, Municipal wastewater effluent characterization and variability analysis in view of an ozone dose control strategy during tertiary treatment: The status in Belgium, Sci. Total Environ. 625 (2018) 1198–1207. https://doi.org/10.1016/j.scitotenv.2018.01.032.

[34] M. Sgroi, P. Roccaro, G. V. Korshin, V. Greco, S. Sciuto, T. Anumol, S.A. Snyder, F.G.A. Vagliasindi, Use of fluorescence EEM to monitor the removal of emerging contaminants in full scale wastewater treatment plants, J. Hazard. Mater. 323 (2017) 367–376. https://doi.org/10.1016/j.jhazmat.2016.05.035.

[35] H. Bader, J. Hoigné, Determination of ozone in water by the indigo method, Water Res. 15 (1981) 449–456. https://doi.org/10.1016/0043-1354(81)90054-3.

[36] C. Liang, C.-F. Huang, N. Mohanty, R.M. Kurakalva, A rapid spectrophotometric determination of persulfate anion in ISCO., Chemosphere. 73 (2008) 1540–3. https://doi.org/10.1016/j.chemosphere.2008.08.043.

[37] R.B. Baird, A.D. Eaton, E.W. Rice, Standard methods for the examination of

water and waste water (23th edition), 2017. https://doi.org/10.1016/0003-2697(90)90598-4.

[38] K.R. Murphy, C.A. Stedmon, D. Graeber, R. Bro, Fluorescence spectroscopy and multi-way techniques. PARAFAC, Royal Society of Chemistry, 2013. https://doi.org/10.1039/c3ay41160e.

[39] Y. Yang, K. Demeestere, S. Van Hulle, Ozone-based advanced oxidation of biologically treated landfill leachate: Oxidation efficiency, mechanisms, and surrogate-based monitoring for bulk organics, J. Environ. Chem. Eng. 9 (2021) 106459. https://doi.org/10.1016/J.JECE.2021.106459.

[40] X. He, S.P. Mezyk, I. Michael, D. Fatta-Kassinos, D.D. Dionysiou, Degradation kinetics and mechanism of β-lactam antibiotics by the activation of H2O2 and Na2S2O8 under UV-254nm irradiation, J. Hazard. Mater. 279 (2014) 375–383. https://doi.org/10.1016/j.jhazmat.2014.07.008.

[41] Y. Ding, X. Wang, L. Fu, X. Peng, C. Pan, Q. Mao, C. Wang, J. Yan, Nonradicals induced degradation of organic pollutants by peroxydisulfate (PDS) and peroxymonosulfate (PMS): Recent advances and perspective, Sci. Total Environ. 765 (2021) 142794. https://doi.org/https://doi.org/10.1016/j.scitotenv.2020.142794.

[42] X. Duan, H. Sun, Z. Shao, S. Wang, Nonradical reactions in environmental remediation processes: Uncertainty and challenges, Appl. Catal. B Environ. 224 (2018) 973–982. https://doi.org/10.1016/J.APCATB.2017.11.051.

[43] L. Gao, Y. Guo, J. Huang, B. Wang, S. Deng, G. Yu, Y. Wang, Simulating micropollutant abatement during cobalt mediated peroxymonosulfate process by probe-based kinetic models, Chem. Eng. J. 441 (2022) 135970. https://doi.org/10.1016/J.CEJ.2022.135970.

[44] H.M. Park, Comparing Group Means: T-tests and One-way ANOVA Using Stata, SAS, R, and SPSS *, (2003). http://www.indiana.edu/~statmathhttp://www.indiana.edu/~statmath (accessed May 30, 2022).

[45] L. Lian, B. Yao, S. Hou, J. Fang, S. Yan, W. Song, Kinetic Study of Hydroxyl and Sulfate Radical-Mediated Oxidation of Pharmaceuticals in Wastewater Effluents, Environ. Sci. Technol. 51 (2017) 2954–2962. https://doi.org/10.1021/acs.est.6b05536.

[46] Vlaamse Milieumaatschappij (VMM), Waterverontreiniging door metalen in 2017, Vlaam. Milieumaatschappij. (2017).

[47] Y. Chen, F. Xiao, Y. Liu, D. Wang, M. Yang, H. Bai, J. Zhang, Occurance and control of manganese in a large scale water treatment plant, Front. Environ. Sci. Eng. 9 (2014) 66–72. https://doi.org/10.1007/s11783-014-0637-1.

[48] A.H. Nielsen, P. Lens, J. Vollertsen, T. Hvitved-Jacobsen, Sulfide-iron interactions in domestic wastewater from a gravity sewer, Water Res. 39 (2005) 2747–2755. https://doi.org/10.1016/j.watres.2005.04.048.

[49] V. Alimohammadi, M. Sedighi, E. Jabbari, Experimental study on efficient removal of total iron from wastewater using magnetic-modified multi-walled carbon nanotubes, Ecol. Eng. 102 (2017) 90–97. https://doi.org/10.1016/j.ecoleng.2017.01.044.

[50] H. Zhang, X. Liu, J. Ma, C. Lin, C. Qi, X. Li, Z. Zhou, G. Fan, Activation of peroxymonosulfate using drinking water treatment residuals for the degradation of atrazine, J. Hazard. Mater. 344 (2018) 1220–1228. https://doi.org/10.1016/J.JHAZMAT.2017.11.038.

[51] E.C. Wert, F.L. Rosario-Ortiz, S.A. Snyder, Effect of ozone exposure on the

oxidation of trace organic contaminants in wastewater., Water Res. 43 (2009) 1005–14. https://doi.org/10.1016/j.watres.2008.11.050.

[52] H. V. Lutze, N. Kerlin, T.C. Schmidt, Sulfate radical-based water treatment in presence of chloride: Formation of chlorate, inter-conversion of sulfate radicals into hydroxyl radicals and influence of bicarbonate, Water Res. 72 (2015) 349–360. https://doi.org/10.1016/j.watres.2014.10.006.

[53] Y. Pang, Z.H. Tong, L. Tang, Y.N. Liu, K. Luo, Effect of humic acid on the degradation of methylene blue by peroxymonosulfate, Open Chem. 16 (2018) 401–406. https://doi.org/10.1515/CHEM-2018-0044/DOWNLOADASSET/SUPPL/CHEM-2018-0044_SM.PDF.

[54] J. Wang, S. Wang, Activation of persulfate (PS) and peroxymonosulfate (PMS) and application for the degradation of emerging contaminants, Chem. Eng. J. 334 (2018) 1502–1517. https://doi.org/10.1016/j.cej.2017.11.059.

[55] M. Nihemaiti, R.R. Permala, J.P. Croué, Reactivity of unactivated peroxymonosulfate with nitrogenous compounds, Water Res. 169 (2020) 115221. https://doi.org/10.1016/j.watres.2019.115221.

[56] Y. Zhou, Y. Gao, J. Jiang, Y.M. Shen, S.Y. Pang, Y. Song, Q. Guo, A comparison study of levofloxacin degradation by peroxymonosulfate and permanganate: Kinetics, products and effect of quinone group, J. Hazard. Mater. 403 (2021) 123834. https://doi.org/10.1016/J.JHAZMAT.2020.123834.

[57] S. Zhang, V. Rouge, L. Gutierrez, J.P. Croue, Reactivity of chromophoric dissolved organic matter (CDOM) to sulfate radicals: Reaction kinetics and structural transformation, Water Res. 163 (2019). https://doi.org/10.1016/j.watres.2019.07.013.

[58] E. Deniere, H. Van Langenhove, S. Van Hulle, K. Demeestere, Improving the

ozone-activated peroxymonosulfate process for removal of trace organic contaminants in real waters through implementation of an optimized sequential ozone dosing strategy, Sci. Total Environ. 856 (2023).

[59] T.M. Hwang, S.H. Nam, J. Lee, J.W. Koo, E. Kim, M. Kwon, Hydroxyl radical scavenging factor measurement using a fluorescence excitation-emission matrix and parallel factor analysis in ultraviolet advanced oxidation processes, Chemosphere. 259 (2020) 127396. https://doi.org/10.1016/j.chemosphere.2020.127396.

[60] L. Yang, J. Hur, W. Zhuang, Occurrence and behaviors of fluorescence EEM-PARAFAC components in drinking water and wastewater treatment systems and their applications: a review, Env. Sci Pollut Res. 22 (2015) 6500–6510. https://doi.org/10.1007/s11356-015-4214-3.

[61] X. Chen, M. Yu, X. He, M. Zheng, B. Xi, Y. Sun, X. Fu, J. Su, Fate of dissolved organic matter substructure in a full-scale wastewater treatment plant by using size exclusion chromatography multi-excitation-emission matrix analysis, J. Clean. Prod. 328 (2021) 129677. https://doi.org/10.1016/J.JCLEPRO.2021.129677.

Table 1. Physical-chemical characteristics of the secondary effluent.

Parameter	**Value**
COD (mg O_2/L)	18.2
Nitrite (mg NO_2-N/L)	< 0.015
Alkalinity (mg/L as $CaCO_3$)	226
Chloride (mg Cl^-/L)	160
Sulfate (mg SO_4^{2-}/L)	79
pH	7.85
Turbidity (NTU) [a]	0.47
IOD (mg/L)[b]	4.2
IOD_{PMS} (mg/L)[b]	5.2

[a] Measured before filtration. [b] The added ozone concentration during determination of IOD and IOD_{PMS} was 8.5 ± 0.1 mg/L.

Table 2. Identification of the PARAFAC components (C1-C4).

	Ex/Em (nm)	**Fluorophore type**	**Reference**
C1	320/410	Humic-like or fulvic acid-like (microbial origin)	[60]
C2	275,365/434	Humic-like or fulvic acid-like (microbial origin)	[60,61]
C3	275,380/484	Humic-like (terrestrial origin)	[60,61]
C4	290/338	Soluble microbial by-products	[61]

Table 3. Location of the inflection point – expressed as a value of surrogate intensity reduction – in the surrogate based models for the prediction of TrOCs removal.

	0.5 min		**30 min**	
	O_3	**O_3/PMS**	**O_3**	**O_3/PMS**
ΔUVA_{254}	21%	31%	22%	32%
$\Delta Fmax_1$	65%	60%	60%	48%
$\Delta Fmax_2$	63%	55%	59%	46%
$\Delta Fmax_3$	62%	49%	49%	45%
$\Delta Fmax_4$	71%	48%	57%	49%

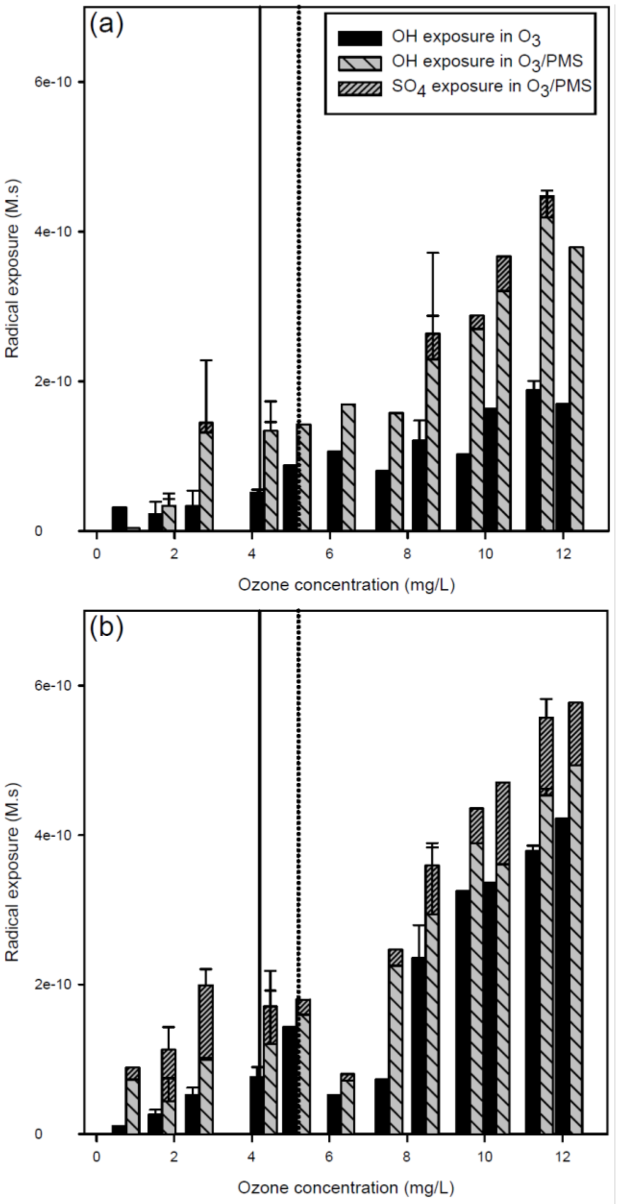

Figure 1. The $^{\bullet}$OH and $SO_4^{\bullet-}$ exposure during O_3 and O_3/PMS after (a) 0.5 min and (b) 30 min of reaction. The error bars represent the standard deviation (n = 2). The vertical solid line and dotted line represent the IOD and IOD_{PMS}, respectively. Conditions: $[O_3]$ = 0 – 12.3 mg/L, [PMS] = 64 mg/L.

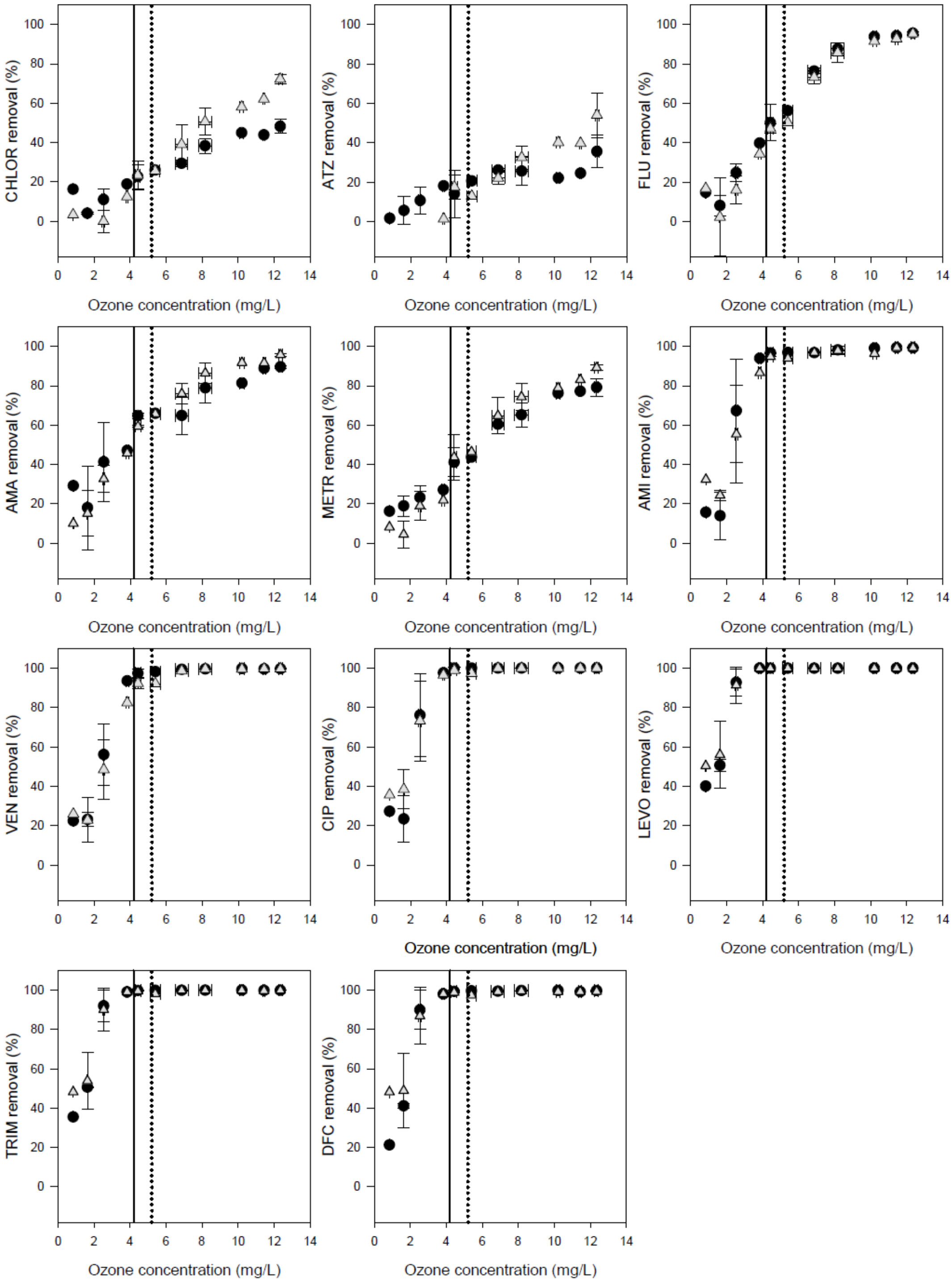

Figure 2. Removal efficiency of the 11 selected TrOCs as a function of the applied ozone concentration after 0.5 min of reaction during O_3 (black circles) and O_3/PMS (grey triangles). A = CHLOR, B = ATZ, C = FLU, D = AMA, E = METR, F = AMI, G = VEN, H = CIP, I = LEVO, J = DCF, K = TRIM. The error bars represent the standard deviation (n = 2).The vertical line and dotted line represent the IOD and IOD$_{PMS}$, respectively. Conditions: [O_3] = 0 – 12.3 mg/L, [PMS] = 64 mg/L, [TrOC] = 1 µg/L.

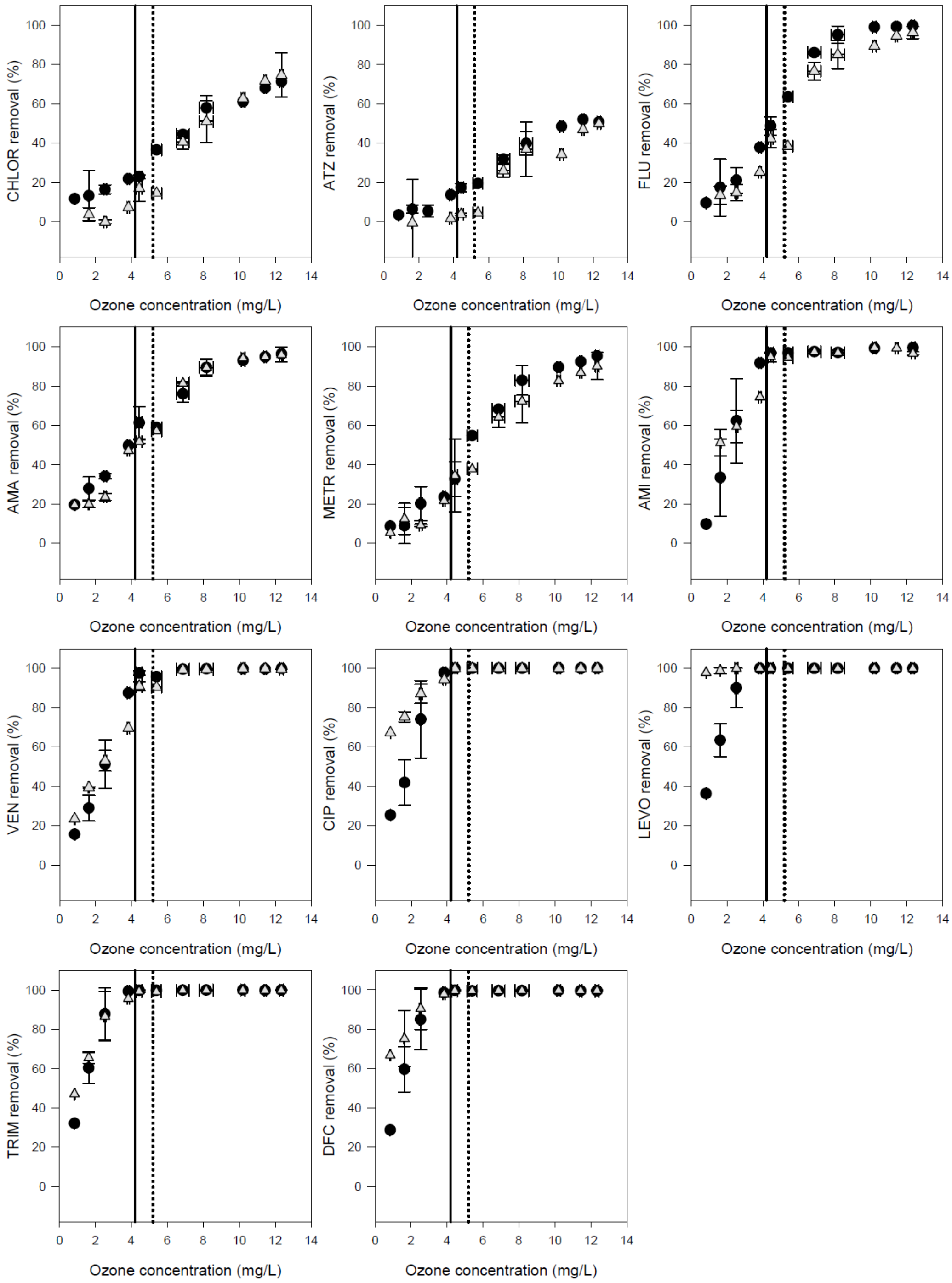

Figure 3. Removal efficiency of the 11 selected TrOCs as a function of the applied ozone concentration after 30 min of reaction during O$_3$ (black circles) and O$_3$/PMS (grey triangles). A = CHLOR, B = ATZ, C = FLU, D = AMA, E = METR, F = AMI, G = VEN, H = CIP, I = LEVO, J = DCF, K = TRIM. The error bars represent the standard deviation (n = 2). The vertical line and dotted line represent the IOD and IOD$_{PMS}$, respectively. Conditions: [O$_3$] = 0 – 12.3 mg/L, [PMS] = 64 mg/L, [TrOC] = 1 µg/L.

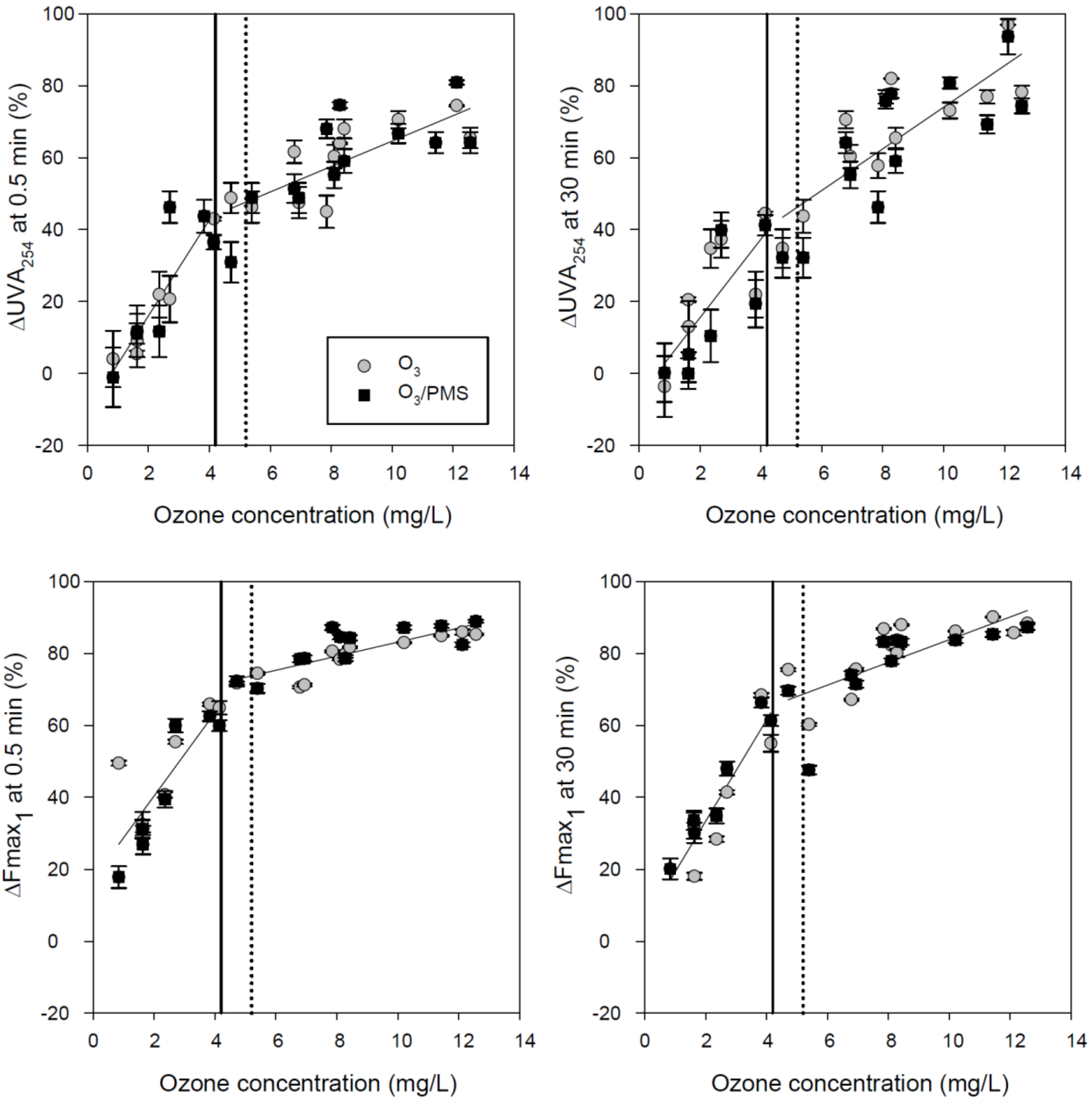

Figure 4. The reduction of UVA$_{254}$ and Fmax$_1$ as a function of the applied ozone concentration after 0.5 and 30 min of reaction, divided in 2 phases. Results are presented for both the O$_3$ (black squares) and O$_3$/PMS (grey circles) process. The vertical line and dotted line represent the IOD and IOD$_{PMS}$, respectively. Conditions: [O$_3$] = 0 – 12.3 mg/L, [PMS] = 64 mg/L.

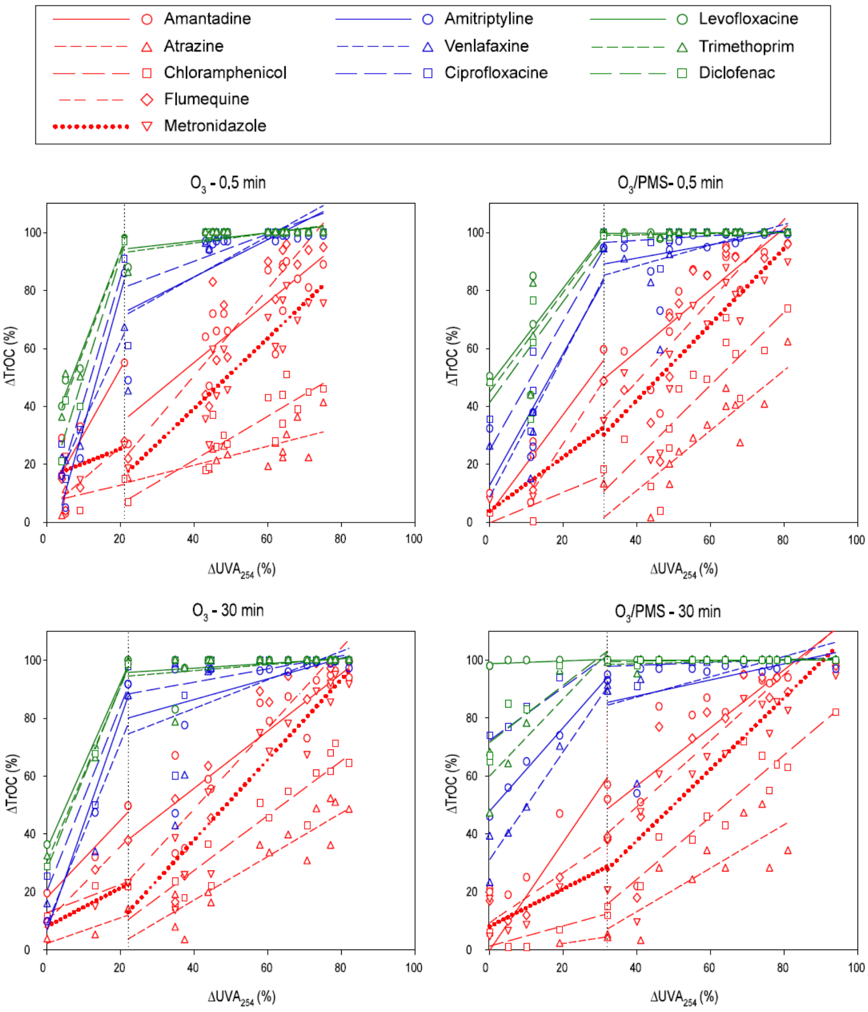

Figure 5. Correlation models between TrOCs removal and ΔUVA_{254}, divided in two phases. The dotted line indicates the inflection point. Models are given for both O_3 and O_3/PMS and at both reaction times (0.5 and 30 min).

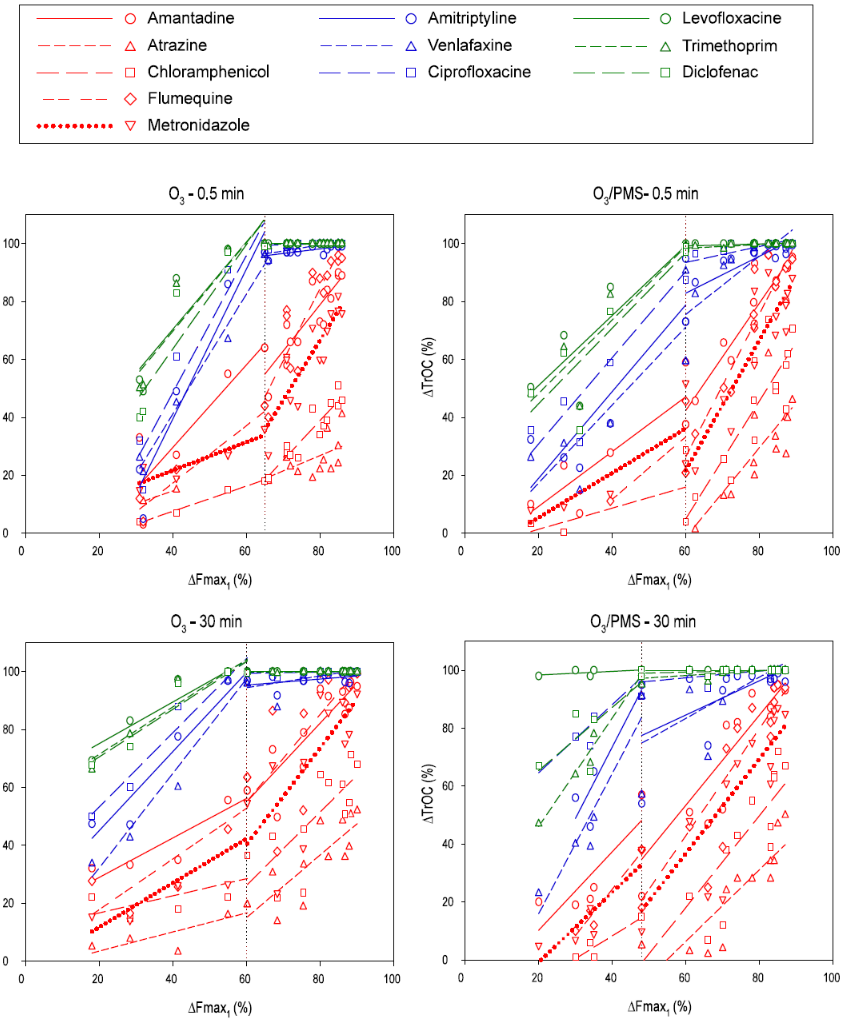

Figure 6. Correlation models between TrOCs removal and ΔFmax$_1$, divided in two phases. The dotted line indicates the inflection point. Models are given for both O_3 and O_3/PMS and at both reaction times (0.5 and 30 min).